MUTATION OF POLARIS, AN INTRAFLAGELLAR TRANSPORT PROTEIN, SHORTENS NEURONAL CILIA

Deependra Mahato, B.S.

Thesis Prepared for the Degree of

MASTER OF SCIENCE

UNIVERSITY OF NORTH TEXAS

August 2005

APPROVED:

Jannon Fuchs, Major Professor
Harris Schwark, Co-Major Professor
Guenter Gross, Minor Professor
Arthur Goven, Chair of the Department of Biological Science
Sandra L. Terrell, Dean of the Robert B. Toulouse School of Graduate Studies

Mahato, Deependra. *Mutation of Polaris, an Intraflagellar Transport Protein, Shortens Neuronal Cilia.* Master of Science (Biology), August 2005, 41 pp., 6 tables, 13 figures, references, 38 titles.

Primary cilia are non-motile organelles having 9+0 microtubules that project from the basal body of the cell. While the main purpose of motile cilia in mammalian cells is to move fluid or mucus over the cell surface, the purpose of primary cilia has remained elusive for the most part. Primary cilia are shortened in the kidney tubules of $Tg737^{orpk}$ mice, which have polycystic kidney disease due to ciliary defects. The product of the Tg737 gene is polaris, which is directly involved in a microtubule-dependent transport process called intraflagellar transport (IFT). In order to determine the importance of polaris in the development of neuronal cilia, cilium length and numerical density of cilia were quantitatively assessed in six different brain regions on postnatal days 14 and 31 in $Tg737^{orpk}$ mutant and wildtype mice. Our results indicate that the polaris mutation leads to shortening of cilia as well as decreased percentage of ciliated neurons in all brain regions that were quantitatively assessed. Maintainance of cilia was especially affected in the ventromedial nucleus of the hypothalamus. Furthermore, the polaris mutation curtailed cilium length more severely on postnatal day 31 than postnatal day 14. These data suggests that even after ciliogenesis, intraflagellar transport is necessary in order to maintain neuronal cilia. Regional heterogeneity in the effect of this gene mutation on neuronal cilia suggests that the functions of some brain regions might be more compromised than others.

ACKNOWLEDGEMENT

I would like to thank Dr. Jannon Fuchs for her guidance on this project and for her critical comments on this thesis. I would also like to appreciate Dr. Harry Schwark for his scientific thoughts during our stimulating discussion. Fabian Dias for his assistance in data analysis and Mahendra Mahato for his support in statistical analysis.

TABLE OF CONTENTS

Page

LIST OF TABLES

LIST OF FIGURES

INTRODUCTION

Background Information

Cilia have been given little recognition compared to other organelles, despite their prevalence throughout the animal kingdom and in some plants (Yoder et al. 2002). Well over two hundred peptides are involved in a cilium's formation, maintenance and function (Dutcher 1995, Haycraft et al. 2001). Motile cilia have nine peripheral doublets of microtubules with a centrally located pair; hence, they have been described as a 9+2 pattern. Despite the fact that cilia have received considerably less attention than other organelles, they have wide range of functions. Olfactory cilia act as chemosensors via specific odorants binding to specific odorant receptors and initiating signal transduction. Motile cilia on epithelial cells in the lungs help move debris out of the lungs and maintain proper milieu for gas exchange by regulating the composition of mucus. Ependymal cells lining the ventricles of the brain and the central canal of the spinal cord also contain motile cilia that maintain the right chemical environment by moving the cerebral spinal fluid. In addition, motile cilia are also required for embryonic patterning (Marzalek et al. 1999). Beating of cilia on the node, a gastulation stage organizing center, creates a leftward extra-embryonic fluid flow that is apparently required for asymmetric distribution of morphogens (Nonaka et al. 1998, Murcia et al. 2000).

Another category of cilia is primary cilia, which are solitary and non-motile. These cilia have nine peripheral doublets of microtubules but are missing the centrally located pair and thus have a 9+0 pattern. Primary cilia have received little attention despite their

pervasive presence throughout the nervous system and other organs. In the nervous system, primary cilia have been localized with the aid of electron microscopy in several regions, including the retinal inner nuclear and ganglion cell layers of guinea pigs and humans (Allen 1965), the lateral geniculate nucleus (Karlsson 1966), the preoptic nucleus of the rat (Peters et al. 1976), and the cerebral cortex (Dahl 1963). Due to the elusive role of primary cilia (Fuchs and Schwark 2004, Pazour 2004, Whitfield 2004), they have been considered as functionless vestigial organelles.

Recent research advances in other cell types have suggested that these primary cilia may have a crucial role as an extrasynaptic signaling device. Although primary cilia are non-motile, they are nonetheless busy transporting large particles called “rafts” back and forth along their length using intraflagellar transport (IFT) (Rosenbaum et al. 1999). In the antegrade transport system, kinesin II motor protein pulls rafts loaded with goods such as receptors, ion channel subparticles, and specific signal enzymes from the centriolar basal body up to the tip of the cilium along the outer microtubule doublets (Kozminski et al. 1993). Similar to the antegrade transport system, the retrograde transport system involves cytoplasmic dynein 1b, (cDHC1b) (Pazour et al. 1999) which carries wastes as well as products of the membrane signaling components down to the basal body from the tip for disposal or further transmission to the cell body (Whitfield 2004). Since protein synthesis does not occur within the cilium (Haycraft et al. 2001), this type of transport system is essential for cilia formation, maintenance, and function.

Mutations that alter the composition or movement of either of IFT lead to defects in cililogenesis and thus hamper ciliary function (Pazour et al. 2000). One such mutation occurs in the transgenic *Oak Ridge polycystic kidney mutation* ($Tg737^{orpk}$) mouse. The

gene product of Tg737 is polaris (Murcia et al. 2000), one of the intraflagellar transport proteins (IFT) that carries cargo via a retrograde transport system using dynein 1b (Pazour et al. 1998). The $Tg737^{orpk}$ allele is an insertional mutation generated by integrating exogenous DNA into an intron (Moyer et al. 1994). This results in a hypomorphic mutation which impairs but does not completely disable protein function. With a homozygous hypomorphic mutation of Tg737 gene, $Tg737^{orpk}$ (-/-) mice have short stunted primary cilia in the kidney, at the embryonic node, and in the retina (Murcia et al. 2000, Taulman et al. 2001, Pazour et al. 2002) when compared to wildtype, $Tg737^{orpk}$(wt). Due to the homozygous mutation in polaris, $Tg737^{orpk}$(-/-)mice develop polycystic kidney disease (PKD), defects in left-right asymmetry, and retinal degeneration (Murcia et al. 2000, Taulman et al. 2001, Pazour et al. 2000).

Studying cultured cells of kidney tubule epithelia has revealed that primary cilia may function as flowmeters via Ca^{2+} influx due to tubular fluid flow (Praetorius and Spring 2001). A mechanoreceptor of primary cilia, polycystin-1 (PC-1) is a large transmembrane protein that protrudes out of the membrane at focal adhesion contacts, which is associated with polycystin-2 (PC-2), a Ca^{2+} permeable cation channel. When the fluid flows over the cell surface of the lumen, the cilium bends, which causes the protein PC-1 that protudes into the lumen to open PC-2, a Ca^{2+} channel, via mechanical pull (Newby et al. 2002, Nauli et al. 2003). It is hypothesized that incoming Ca^{2+} triggers release of additional Ca^{2+} from internal stores, which may in turn spread to adjacent cells, perhaps via IP_3 diffusing through gap junctions to adjacent cells, which would further release Ca^{2+} from their internal stores (Praetorius and Spring 2001). This relay of the Ca^{2+} message to adjacent cells causes specific physiological responses. In kidney,

the primary cilia are necessary to maintain the specific chemical milieu of the tubular fluid (Yoder et al. 2002). Disruption of either PC-1 or PC-2 complex leads to formation of epithelia-lined cysts throughout the nephron and predominantly in the collecting duct (Nauli et al. 2003).

Based on the kidney model, the question arises whether primary cilia of neurons also respond to fluid movement in the extracellular matrix or have completely different function. Although the primary cilia in the kidney extend into the passing urine, the neuronal cilia are not long enough to dip into the cerebrospinal fluid. Given their ubiquitous location in the brain, these neuronal cilia probably function somewhat differently in the CNS (Handel et al. 1999). The observation that somatostatin receptor type 3 (sst3) is largely confined to the primary cilia of neurons (Handel et al. 1999), suggests some evidence that these organelles may have specific roles in detecting external sources of somatostatin and may serve as an interface with the extracellular environment, similar to the role of olfactory cilia. Furthermore, it is likely that these sst3 receptor components are specifically sent from the region of the basal body of cilia using the IFT. Sst3 immunoreactive neuronal cilia have been identified in one or more regions within each of the following areas of the rat central nervous system: the main olfactory bulb, cerebral cortex, hippocampus, basal ganglia, septal and basal forebrain regions, amygdala, thalamus, hypothalamus, midbrain, pons, medulla oblongata, cerebellum, and spinal cord (Handel et al. 1999). Furthermore, since the brain is densely packed with neurons and glial, these relatively long 4-8 μm primary cilia might be the most effective organelle in responding to local somatostatin hormones either released from blood stream or locally (Whitfield 2004).

Since polycystic kidney disease (PKD) can be caused by defective or absent renal primary cilia, numerous studies have been carried out to investigate the connection between PKD and cilia. The gene product of Tg737^{orpk} gene, polaris, contains a tetratricopeptide repeat (TPR), which has been shown to play an active role in the ciliogenic pathway through protein-protein interactions (Nakanishi et al. 2001). Polaris solubility and localization to the basal body and cilia axoneme change dramatically during cilia formation (Yoder et al. 2002). In addition, characterizations of mutant Tg737^{orpk} mouse kidney have suggested that stunted cilia or absent cilia can compromise their function as sensors. Due to the fact that polaris contains a 10-TPR motif (Pazour 2000), which is thought to be involved in protein-protein interactions, it may either function as part of the transport system described above (IFT) or as part of the cargo that is transported during the ciliogenesis. The disruption of the IFT system in the Tg737^{orpk} mouse causes cargo items to accumulate and ultimately leads to cysts (Pazour et al. 1999). Previous Northern blot analysis suggests polaris is ubiquitously expressed as multiple spliced transcripts in mice (Yoder et al. 1995). Several types of cells are heavily dependent on polaris for ciliogenesis and maintaince as indicated by stunted or absent cilia in renal tubules, distal bronchioles and in the trachea, sperm, and ependymal lining the ventricles of mutant Tg737^{orpk} mice (Taulman et al. 2001). Cells that do not have normal cilia in homozygous mutant Tg737^{orpk} mouse can be corrected by re-expression of the wild-type Tg737 gene, which further establishes the crucial role of polaris in development of cilia (Yoder et al. 2002).

In addition to ependymal cells, polaris expression is also present in other regions of the adult brain such as the hippocampus and the dentate gyrus (Taulman et al.

2001). While cilia length in rat brain has been determined using $G\alpha_{11}$-immunohistochemistry (Hughes et al. 2002), cilia length in mouse brain has not yet been published. Because the role of neuronal cilia has remained elusive, it is important to determine whether polaris serves the same role in the development of these neuronal cilia as it clearly does in renal primary cilia. Preliminary reports have indicated that some neuronal cilia appear to be absent in mutant $Tg737^{orpk}$(-/-) mice using sst3 immunolocalization (Fuchs and Schwark 2004). This suggests that polaris may serve a similar role in neuronal cilia either as a protein required for development or maintenance. In addition regional heterogeneity among brain regions has not been assessed quantitatively. Therefore, it is also our interest to determine how polaris mutation affects cilium length in selected brain regions. By identifying brain regions where cilia are absent or severely shortened, further studies can be carried out to determine what role neuronal cilia play in the function of these regions. Since each region of the brain has a specific physiological function, the role of cilia in these uniquely functioning brain regions can be evaluated. Once certain brain regions that are severely dependent on polaris for maintenance of cilia has been identified, a complete knockout of polaris in those regions can be carried out to further assess the role of neuronal cilia. While it is known that polaris mutation reduces cilium length in kidney tubule epithelial cells, quantification of polaris effects have not been published for the brain. Therefore it is our primary concern to quantitatively study the effects of polaris on cilia length and on the neurons that are missing cilia.

Given that loss of cilia would probably entail a decrease in sst3 receptors, neurons from $Tg737^{orpk}$ (-/-) mice may be deficient in their ability to respond to

somatostatin, and thus perhaps make them vulnerable to neurodegenerative disease associated with excitotoxicity. Somatostatin has been shown to hyperpolarize hippocampal pyramidal neurons (Schweitzer et al. 1993), thalamic reticular nucleus (Sun et al. 2002) and other brain regions. Therefore the lack of somatostatin effect may cause excitotoxicity within the central nervous system. Consequently, the first step in determining whether any compromise has occurred in neuronal function in Tg737^{orpk}(-/-) mice is to first quantitatively determine if cilium length and numerical density has been reduced.

Specific Aims

The aim of this project was to investigate primary cilia in Tg737^{orpk} wildtype and Tg737^{orpk} mutant mice via immunolocalization of primary cilia in the central nervous system using the sst3 antibody. The specific investigative goals included:

1. Surveying the abundance of sst3 –immunoreactive cilia in various brain regions of Tg737^{orpk} wildtype and Tg737^{orpk} mutant mice.
2. Comparing sst3 immunoreactive cilia length and percentage of ciliated neurons in Tg737^{orpk} mice versus wildtype in mouse in specific brain regions: granular layer (GrL) and internal plexiform layer (IPL) of olfactory bulb, layer 2 of piriform cortex, claustrum, hilus of the dentate gyrus, and ventromedial nucleus of the hypothalamus (VMH).
3. Examining the developmental change in sst3 –immunoreactive cilia in Tg737^{orpk} mutant and wildtype mice between postnatal days 14 and 31.

MATERIALS AND METHODS

Subjects

Subjects were the progeny of Tg737$^{orpk\ (+/-)}$ breeding pairs of mice provided by Noel Murcia (Case Western Reserve University). The heterozygous Tg737 ^{orpk} mice yielded homozygous Tg737 $^{orpk(-/-)}$ mutants in a somewhat less than Mendelian ratio.

Antibodies

The primary antibody used was rabbit monoclonal sst3 antibody (SS-830; Gramsch Laboratories, Schwabhausen, Germany) directed against the C-terminal amino acid sequence (TAGDKASTLSHL) of rat or mouse somatostatin receptor type 3 coupled to KLH. The antibody was packaged in 250 µl of lyophized antiserum, which was reconstituted with 250µl of water and stored in aliquots at -20^{o} C until used.

Tissue Preparation

Mice were deeply anesthetized with 20% urethane solution (1 ml urethane per 100 g body weight, i.p.) and then transcardially perfused with a 0.9% saline solution followed by a 4% paraformaldehyde solution in 0.1 M phosphate buffer at pH 7.6. Brains and spinal cord were rapidly removed, and then post-fixed in the same fixative solution for 2 hour at 4 ^{o}C. The tissues were then cryoprotected in 30% sucrose for

approximately 48 hour, and frozen in -80 ^{o}C isopentane. The brain tissues were then stored at -80 ^{o}C until used.

Serial Sections Though the Mouse Brain

Frozen tissue was sectioned at a thickness of 40 μm using a sliding microtome. The sections were collected in Tris-buffered saline (TBS), pH 7.6. In order to obtain a series of sections throughout the whole adult mouse brain, coronal sections were taken through an entire brain and stored in cryoprotectant solution (30% glycerol and 30% ethylene glycol in 0.1 M phosphate buffer) at -20^{o} C for no longer than three months. Every sixth section was then processed for immunohistochemistry.

Immunohistochemistry

Selected tissue sections were removed from cryoprotectant solution and rinsed in TBS three times. Sections were then submerged in a pre-incubation solution comprised of TBS with 5% normal goat serum (NGS) and 0.1% Triton X-100 for 30 minute at room temperature. All incubations were performed under continuous gentle agitation. Tissue sections were then incubated with the primary sst3 antibody at 1:1500 dilutions in pre-incubation solution overnight at room temperature. Upon completion of incubation in the primary antibody, tissue sections were washed in TBS three times for 15-minutes each, followed by a 15-minute rinse in pre-incubation solution, and then incubated with secondary antibody biotinylated (goat anti-rabbit; Jackson ImmunoResearch

Laboratories) at a 1:1000 dilution for 1 hour in pre-incubation solution at room temperature. After two 15-minute rinses in TBS, the tissue sections were biotin amplified by processing them in ABC solution (50 μl of Vector Standard A and B solutions in 2.5 ml of TBS with 1% NGS). Tissue sections were then washed in two 15-minute rinses of TBS before being placed in DAB solution (2.5 mg 3,3'-diaminobenzidine and 2 μl of 50% hydrogen peroxide in 5 ml TBS). Tissue sections were allowed to react in DAB solution for 2 minutes or until a faint color change to brown was detected. This was followed by two 15-minute TBS rinses. Tissue sections were mounted onto subbed slides and vacuum dehydrated overnight. The tissue sections were rehydrated to prepare them for counterstaining by placing them first in 70% ethanol followed by 50% ethanol for 10 minutes and a brief dip in dH_2O. The tissue sections were then counterstained with thionin (1.25g thionin, 100 ml of 1N acetic acid, 18 ml 1N NaOH, 382 ml dH_2O) and differentiated in an acidified 95% ethanol solution. The slides were then further dehydrated by being placed in a series of ethanol solutions (50%, 70%, 95%, 100%) and cleared in three consecutive changes of xylenes solutions. The slides were immediately cover slipped with DPX mounting medium and left to dry for at least 4 hours.

Immunofluorescence

All the steps up to and including primary incubation were followed as described above. Upon completion of incubation in the primary antibody, tissue sections were washed in TBS three times for 15 minutes each, followed by a 15 minute rinse in pre-

incubation solution, and then incubated with Alexa Fluor 588 secondary antibody (goat anti-rabbit; Jackson ImmunoResearch Laboratories) at a 1:1000 dilution for 1 hour in pre-incubation solution at room temperature in darkness. This was followed by two 15-minute washes in TBS and incubation in Neurotrace fluorescent Nissl stain (N-21480; Molecular Probes) at 1:500 dilution for 20 minutes. The tissues were washed for 10 minutes in 0.1% Triton X-100 in TBS. After the final wash the tissues were air dried, mounted with ProLong Antifade (P-7481, Molecular Probes) and stored at 0 ^{o}C in the dark.

Data Analysis

Sections that were immunohistochemically processed were examined for the presence of immunoreactive cilia via light microscopy. Specific regions of the hilus of the dentate gyrus, cortex, olfactory bulb, hypothalamus, superior colliculus, and hippocampus were chosen as examples of neuronal cilia length. Within each of these selected regions, approximately 30-150 cilia and 100-400 cells were chosen from several fields of view and from several sections and were drawn separately with the aid of a camera lucida. Cilia selected for drawing were those that lay horizontally across the plane of the section such that their entire length could be brought into focus in same focal plane. The neurons selected for drawing were ones with nuclei and nucleoli present within the 40-μm section.

The drawings were digitized (Adobe Photoshop 6.0) and analyzed using image-analysis software (AIS 60 Rev. 1.0, Imaging Research Inc.). Statistical analysis was

carried out by using SAS software. For each set of data, it was determined whether the data had normal distribution (Shapiro-Wilk test) and equal variance. If the data had normal distribution and equal variance a parametric, two-tailed independent t-test was used to compare sample means between two regions and analyses of variance (ANOVA) were used to compare sets of data. Data sets were log transferred if necessary to meet parametric assumptions. The null hypothesis that no difference exists between the two sample means was tested at the $\alpha = 0.05$ significance level. If data sets were normal but unequal in variance, variance adjusted probability value was used for comparison. The non-parametric matched pair Wilcoxin test was performed if data were not normal even after log transformation.

RESULTS

Immunolocalization of Neuronal Cilia in Adult Tg737^{orpk} Mouse

Tissue sections from 31-day-old Tg737^{orpk}(wt) and Tg737^{orpk}(-/-) mouse brains were analyzed for the presence of sst3-immunoreactive neuronal cilia using rabbit anti-mouse sst3 antibody. As described in Handel et. al (1999), one sst3-immunoreactive cilium was observed almost ubiquitously on each neuron in the majority of brain regions throughout the central nervous system (CNS) of mouse brain. Each region was identified using a stereotaxic altas of the mouse brain (Paxinos and Watson 1990) and was evaluated for the presence of cilia. The number of cilia in each field of view was estimated as follows: Regions that had no cells with cilia were labeled (----), regions that had approximately 1-4 cells with cilia per field of view were labeled (+), 4-10 cells with cilia were labeled (++), 10-20 were labeled (+++), and region higher than 20 was labeled (++++). Regions that were labeled as having a high percentage of cilia were those in which almost all cells possessed a cilium. Regions such as IPL layer of olfactory bulb, hilus of the dentate gyrus, ventromedial hypothalamic nucleus (VMH), and piriform cortex were labeled (++++) to indicate a high numerical density of cilia, while most regions in pons, medulla, and basal ganglia were labeled (+) to indicate sparse cilia. In addition to determining the presence or absence of sst3-immunoreactive cilia, each region was evaluated in terms of cilium length (Table 1). Each region was evaluated qualitatively by simple observation and labeled according to whether cilia were estimated to be: short ($x < 3$ μm), medium ($4\mu m < x < 5\mu m$), long ($5\mu m < x < 7\mu m$),

or very long (x > 7μm). Regions such as the ventromedial hypothalamic nucleus and superior colliculus were labeled very long, while other regions such as CA1 and substantia nigra were labeled medium. In comparison to cilia in the wildtype, neuronal cilia in the mutant were either (1) absent in some neurons, (2) apparently absent in all neurons, or (3) significantly shortened. Although there was a dramatic decrease in the percentage of ciliated neurons in most regions of the brain, certain regions such as hilus of dentate gyrus and pyramidal layers of hippocampus had an especially substantial decrease. Brain regions such as piriform and VMH were considerably affected in terms of neuronal cilium length. Regions that are labeled in bold were selected for further studies.

Immunolocalization of neuronal cilia in the adult mouse CNS				
	Tg737^{orpk} (wt)		**Tg737^{orpk} (-/-)**	
Telencephalon	Presence	Length	Presence	Length
Olfactory Bulb				
mitral cell layer	++++	long	++	short
internal plexiform layer	**++++**	**long**	**++**	**short**
anterior olfactory nucleus	+++	long	++	
granular layer	**++++**	**long**	**++**	**short**
granular cell layer	++++	long	++	short
Cerebral Cortex				
temporal	++	long		
cingulate	++	long	++	short
retrosplenial agranular corex	++	long	+	short
retrosplenial granular corex	++	long		
piriform	**+++**	**long**	**++**	**short**
insula	+++	long	----	short
tenia tecta	+++	long	----	
prelimbic cortex	++	short	+	short
motor cortex	++	long	+	short
primary auditory cortex	++	long	+	short
secondary auditory cortex	++	long	+	short
primary visual cortex	++	medium	+	short
secondary visual cortex	++	medium	+	short
primary somatosensory cortex	++	long	+	short
secondary somatosensory cortex	++	long	+	short
Hippocampal Formation and Associated Areas				
CA1	+++	medium	----	
CA2	+++	medium	----	
CA3	+++	medium	+	medium
hilus of the dentate gyrus	**++++**	**long**	**++**	**medium**
granular layer of the dentate gyrus	----			
presubiculum	+++	long	+	short
parasubiculum	+++	long	+	short
subiculum	+++	long	+	short
medial eminence	++	long		
Basal Ganglia				
caudate putamen	----		----	
nucleus accumbens	----		----	
globus pallidum	----		----	
claustrum	**+++**	**long**	**++**	**short**
ventral pallidum	----		----	
subthalamic nucleus	----		----	
dorsal endopiriform nucleus	+++	long	++	short
Amygdala				
basolateral nuclear group	----		----	
basomedial amygdaloid nucleus	++	long	+	short
posterolateral cortical amygdaloid nucleus	----		----	
Septum				
lateral septal nucleus	+++	long	+	short

Diencephalon				
Thalamus				
lateral geniculate nucleus	+	medium	----	
medial geniculate nucleus	+	medium	----	
posterior thalamic nuclear group	----		----	
Hypothalamus				
preoptic nuclear group	----		----	
mammillary nuclear group	----		----	
ventromedial hypothalamic nucleus	**+++**	**very long**	**+**	**medium**
lateral hypothalamic area	+++	very long	+	short
dorsomedial hypothalamic nucleus	+++	very long	+	short
arcuate hypothalamic nucleus	++++	very long	+	medium
Mesencephalon				
superior colliculus	++	medium	++	short
inferior colliculus	++	medium	----	
oculomotor nuclear group	++	medium	----	
midbrain reticular formation				
periaqueductal gray	++	long	----	
interpeduncular nucleus	++	long	+	short
ventral tegmental area			+	short
substantia nigra	++	medium	+	short
Myelencephalon				
Medulla Oblongata				
vestibular nucleus	++	long	----	
cochlear nucleus	++	long	----	
medullary reticular nucleus				
solitary nucleus	++	long	----	
prepositus nucleus	++	medium	----	
inferior olivary complex				
Spinal Cord				
dorsal horn	++	long	+	short
ventral horn	++	long	+	short

Table1. Distribution of Numerical Density and Length of Neuronal Cilia in Wildtype Compared to Mutant Tg737^{orpk} Mice

Cilia were immunolocalized in most of the regions that was surveyed. In each field of view regions that had no cells with cilia were labeled (----), regions that had 1-4 cells with cilia were labeled (+), 4-10 cells with cilia (++), 10-20 cells were labeled (+++), and anything higher than 20 were labeled (++++). In addition the lengths of ciliated neurons are represented by short ($x < 3$ µm), medium (4µm < x<5µm), long (5µm < x< 7µm), and very long ($x > 7$µm).

Development of Sst-3 Neuronal Cilia

Neurons in the granular cell layer (GrL) of the olfactory bulb were selected for further study on the basis of a high density of cilia, and the ventromedial hypothalamic nucleus (VMH) was selected because it had the long cilia. Neuronal cilia in P14 and P31 mice were compared in six brain regions: GrL and internal plexiform layer (IPL) of the olfactory bulb, layer 2 of the piriform cortex, hilus of the dentate gyrus, VMH, and claustrum. In addition, cilia length varied across regions within each age group. Cilium length increased significantly between P14 and P31 wildtype, in layer 2 of the piriform cortex, the hilus of dentate gyrus, VMH, and claustrum (Table 2, Fig. 1A). The same four regions showed the opposite change in mutant mice (Table 2, Fig. 1B). As shown in Table 3A, cilia length was reduced in homozygous mutant by 39.2% in P14 mice and by 49.2% in P31 mice averaged across all 6 brain regions (see also Fig 2A). Polaris mutation not only had a larger effect on cilia length but also on percentage of ciliated neurons in the P31 mouse than in the P14 mouse (Fig 2B). The percentage of ciliated neurons was reduced by an average of 42.9% in P14 mice while they were reduced by an average of 71.9% in P31 mice (Table 3B, Fig. 2B).

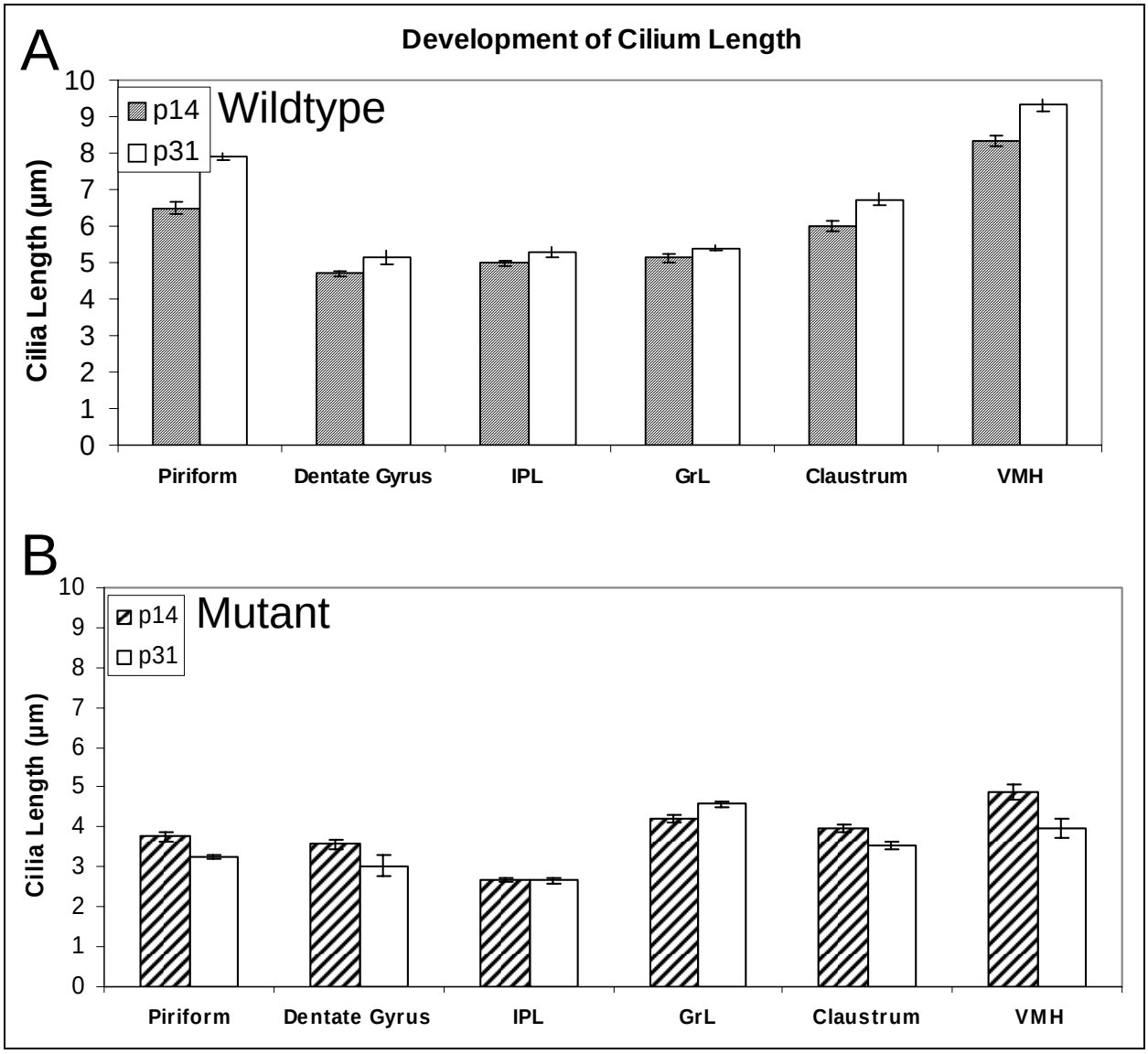

Figure 1. Development of Cilium Length, P14 vs P31. Comparison of Cilium Length Between Postnatal Day P14 and 31 in Various Regions of Wildtype Tg737^{orpk} (A) and Mutant Tg737^{orpk} (B). Shown are the mean ± SEM

In wildtype (A) cilium length increased from P14 to P31, whereas in the mutant (B) cilium length was significantly shorter on P31 than P14, in all brain regions except for internal plexiform layer (IPL) and granular layer (GrL) of the olfactory bulb (Table 3). VMH was especially affected by the Tg737^{orpk} mutation as the cilium length decreased from 9.3 ± 1.8 µm in wildtype to 3.9 ± 1.1 µm in Tg737^{orpk} mutant ($P < 0.0001$).

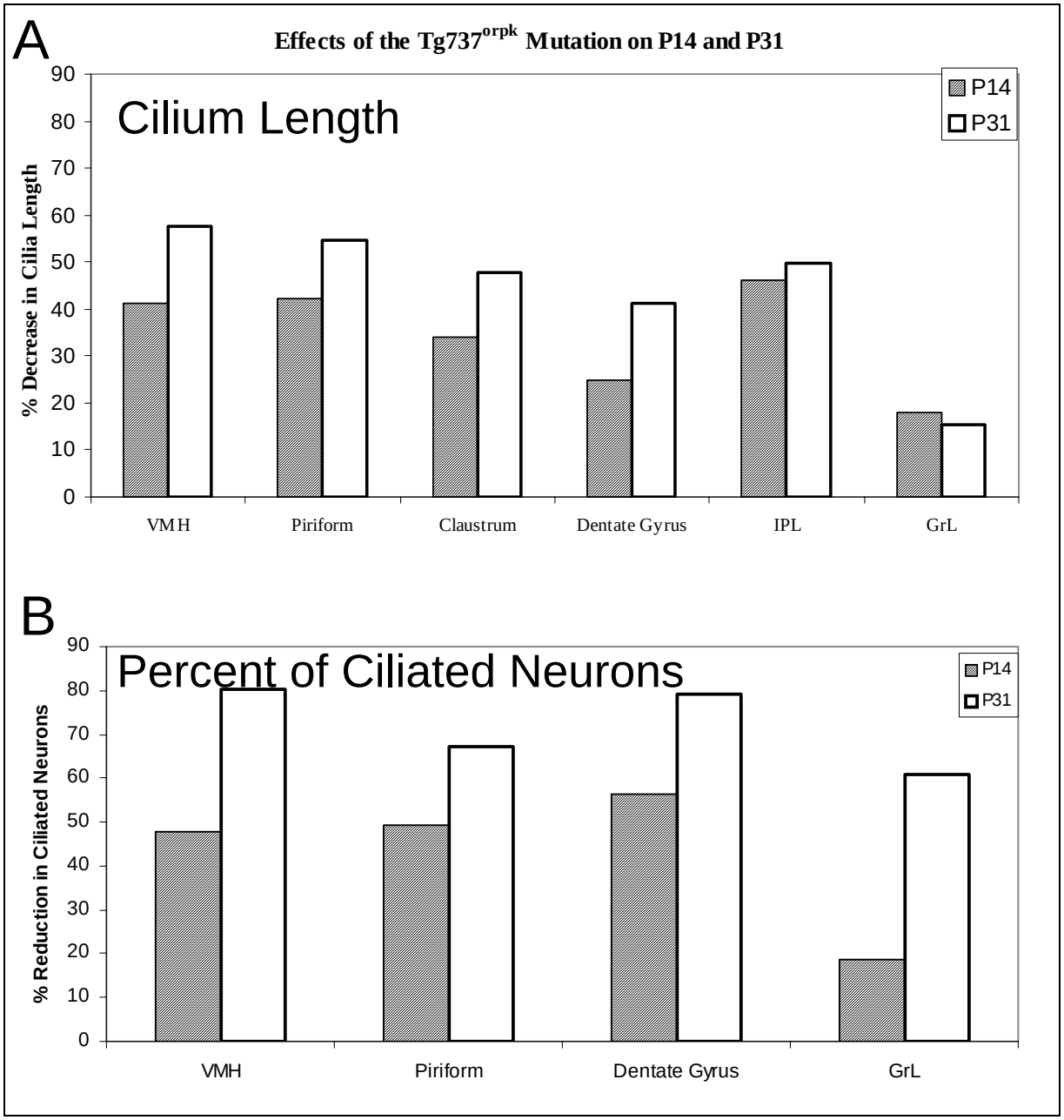

Figure 2. Effect of the Tg737^{orpk} Mutation on Cilium Length (A) and Percent of Ciliated Neurons (B) on P14 and P31

There was a greater percentage decrease in cilium length (A) as well as percentage reduction in ciliated cells (B) on P31 than on P14. The effect of polaris mutation on cilium length was especially prominent in the VMH and ciliated neurons of GrL. Shown are the mean ± SEM.

CNS Region	Wildtype	Mutant
VMH	p < 0.0001	p < 0.0063
piriform	p < 0.0001	p < 0.0001
claustrum	p < 0.0013	p < 0.0011
dentate gyrus	p < 0.0321	p < 0.0309
GrL	p < 0.0655	p < 0.0054
IPL	p < 0.1154	p < 0.1814

Table 2: Cilium length increased between P14 and P31 wildtype, (piriform, dentate gyrus, VMH, and claustrum), while decreased in P31 compared to P14 in those same regions (see also Fig. 2).

A

CNS Region	P14	P31
VMH	41.4	57.6
piriform	42.1	54.7
claustrum	34	47.8
dentate gyrus	25	41.4
GrL	47	44.4
IPL	45.9	49.6
Mean	**39.23**	**49.25**

B

CNS Region	P14	P31
VMH	47.7	80.4
piriform	49.3	67.1
dentate gyrus	56.3	79.1
GrL	18.6	60.9
Mean	**42.9**	**71.9**

Table 3. Percentage Reduction in Cilium Length (A) and Ciliated neurons (B) in Tg737^{orpk} Mutant Compared to Wildtype on P14 and P31

Cilium Length in Tg737^{orpk} Wildtype and Mutant

On both P14 and P31, neuronal cilium length decreased in the Tg737^{orpk} mutant relative to wildtype, in all regions that were analyzed (Fig. 3). Reductions in cilium length as well as in numerical cilia density are clearly shown in Figures 6-8. Although cilium length in the P31 wildtype ranged from 4.3 ± 0.9 µm (IPL) to 9.3 ± 1.8 µm (VMH), the cilia length in the mutant ranged from 2.4 ± 0.7 µm (IPL) to 3.9 ± 1.1 µm (VMH) (Table 4B). Similarly, on P14 the cilium length in the wildtype ranged from 5.1 ± 0.9 µm (IPL) to 8.3 ± 0.8 µm (VMH), but in the mutant only ranged from 2.8 ± 0.4 µm (IPL) to 4.9 ± 0.8 µm (VMH) (Table 4A). In addition many cilia in mutant Tg737^{orpk} were absent or too short to be recognized. The shortest cilium measured was 1.8 µm in P31 IPL region. While there probably were cilia shorter than 1.8 µm, these cilia were most likely overlooked.

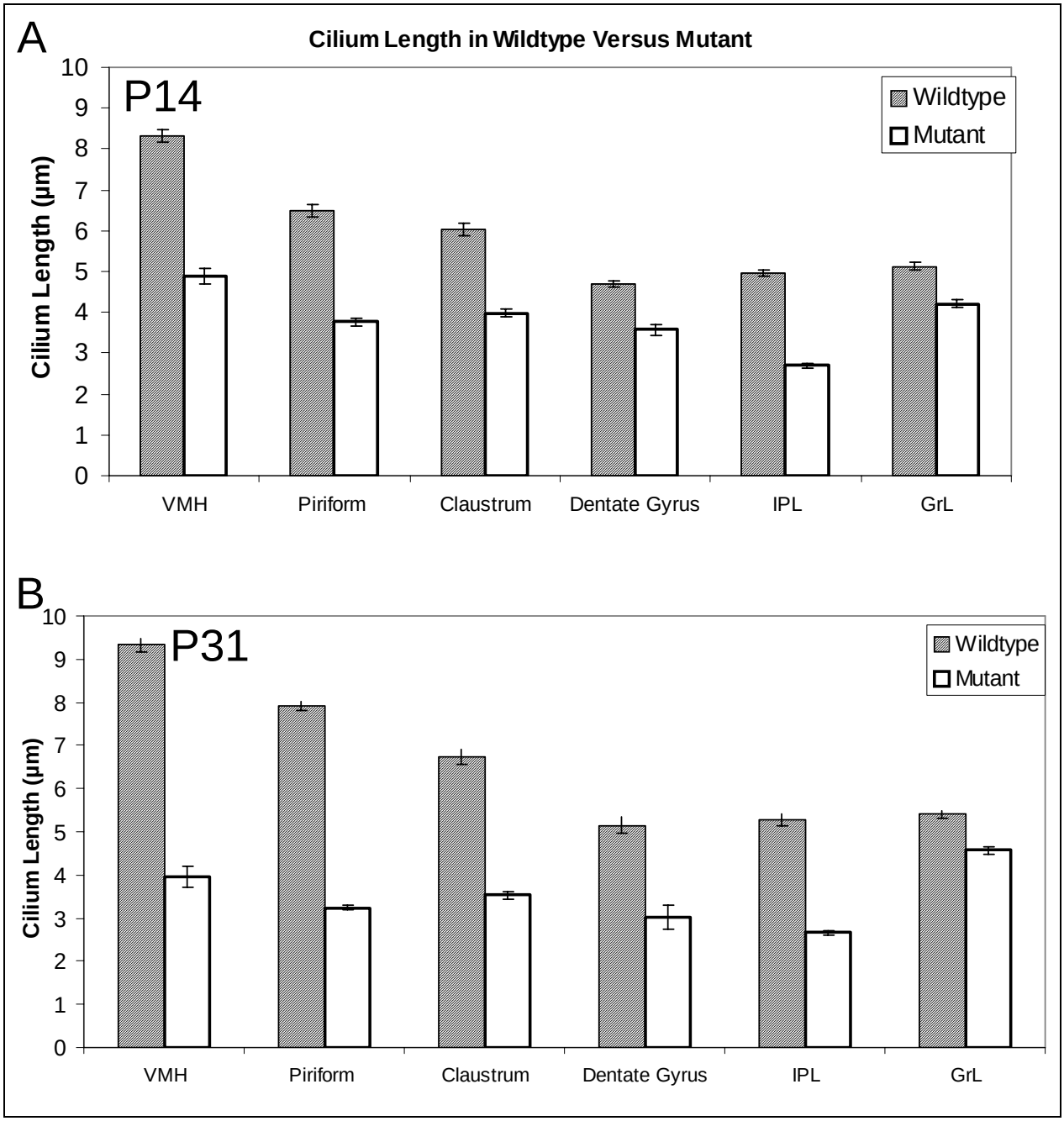

Figure 3. The Tg737^{orpk} mutation shortened cilia significantly on both P14 (A) and P31 (B), in all six regions (see Table 3 for p-values). Shown are the mean ± SEM.

A P14

CNS Region	Wildtype Cilium length (μ)	S.D.	n	Mutant Cilium length (μ)	S.D.	n	p-value
Olfactory Bulb							
GrL	5.13	0.93	72	4.2	0.62	41	< 0.0001
IPI	4.98	0.77	56	2.69	0.48	77	< 0.0001
Cerebral Cortex							
piriform	6.49	1.15	49	3.76	0.63	33	< 0.0001
Hippocampal Formation							
dentate gyrus	4.7	0.66	59	3.57	0.69	34	< 0.0001
Basal ganglia							
claustrum	6.02	1	49	3.98	0.5	32	< 0.0001
Hypothalamus							
VMH	8.32	0.8	29	4.88	0.83	18	< 0.0001
Pons							
cochlear nuclei	7.31	1.45	18	N/A	N/A	N/A	
Cerebellum							
vestibular nucleus	7.44	1.04	19	N/A	N/A	N/A	

B P31

CNS Region	Wildtype Cilium length (μ)	S.D.	n	Mutant Cilium length (μ)	S.D.	n	p-value
Olfactory Bulb							
GrL	5.4	1.15	256	4.57	0.59	46	< 0.0001
IPI	5.28	1.17	75	2.65	0.59	39	< 0.0001
Cerebral Cortex							
piriform	7.91	1.23	151	3.24	0.56	84	< 0.0001
Hippocampus							
dentate gyrus	5.15	1.21	42	3.03	0.99	15	< 0.0001
Basal ganglia							
claustrum	6.73	1.36	71	3.53	0.54	31	< 0.0001
Amygdala							
basomedial nucleus	5.98	1.34	64	N/A	N/A	N/A	
Hypothalamus							
VMH	9.32	1.81	115	3.97	1.09	21	< 0.0001
Midbrain							
superior colliculus	8.99	1.46	59	3.69	0.57	21	< 0.0001

Table 4. Cilium length in various regions of the brain from $Tg737^{orpk(wt)}$ and $Tg737^{orpk(-/-)}$on P14 (A) and P31 (B)

Since the GrL of the olfactory bulb continues to receive new neurons even in adulthood through the rostral migratory stream (Luskin 1993), these neurons were compared with neurons in the IPL where the neurons are probably more differentiated or at least older. On P14, there was no statistical difference between these regions in the wildtype (GrL 5.13 ± 0.93 μm and IPL 5.00 ± 1.21 μm, $p=0.41$, but in the mutant, the cilia in GrL were longer than in the IPL, 4.2 ± 0.62 μm and 2.69 ± 0.48 μm, respectively $p < 0.0001$ (Table 4, Figs. 4 and 9). Similarly on P31, there was no statistical difference in the wildtype GrL 5.40 ± 1.15 μm and IPL 5.2 ± 1.2 μm ($p = 0.37$), but there were statistical differences in the mutant (GrL 4.57 ± 0.09 ± 0.06 and IPL 2.66, $p < 0.0001$. Furthermore, mutants showed much greater reduction in cilium length in the IPL compared to GrL on both P14, (47.8% and 16.8%, respectively) as well as on P31, (49.4% and 15.3%, respectively) (Fig. 2B).

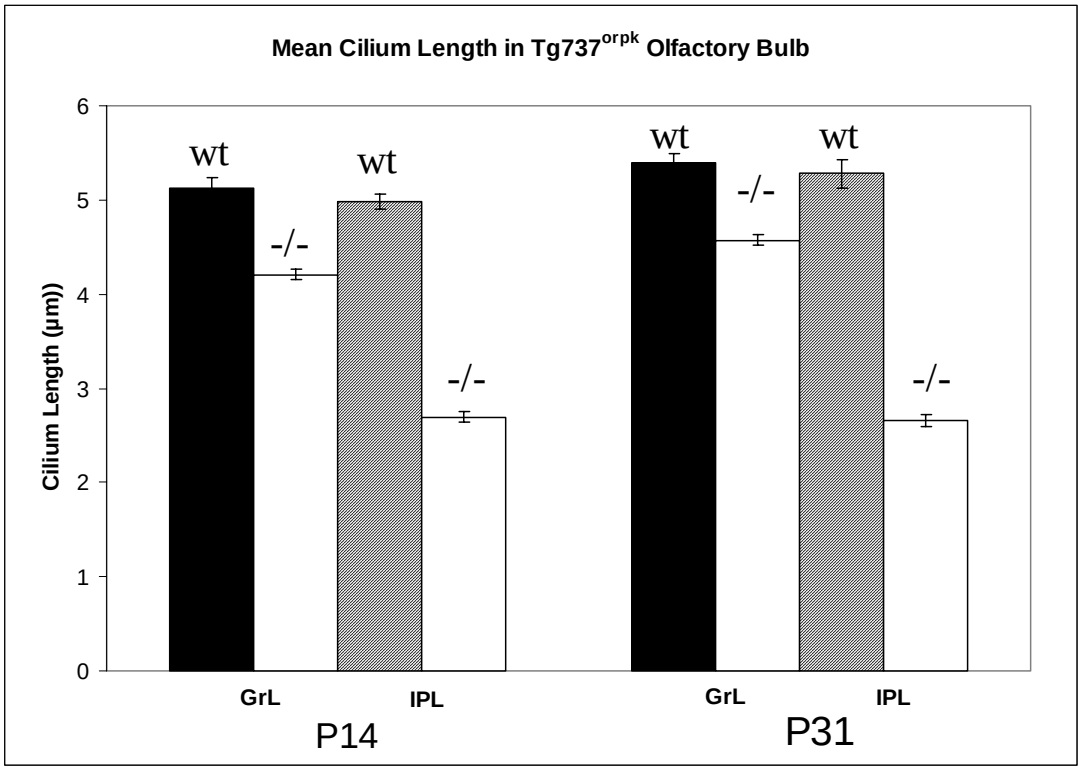

Figure 4: Cilium Length in IPL and GrL of the Olfactory Bulb in wildtype and mutant on P14 and P31. Shown are the mean ± SEM

While there was no statistical difference in cilium length between wildtype Tg737^{orpk} GrL and IPL on P14 ($P < 0.41$) and P31 ($P < 0.38$), there was a much greater decrease in cilium length in mutant Tg737^{orpk} IPL than in GrL on both P14 ($P < 0.0001$) and P31 ($P < 0.0001$).

Cilium Length in Relation to Cell Size

In order to determine whether cell size is related to cilium length, cell size was determined in four regions: VMH, GrL, layer 2 of piriform cortex, and hilus of the dentate gyrus. It has been previously reported that there was no correlation between mean cilium length and mean cell size across regions of the adult rat brain (Hughes 2002). Our findings are in agreement with that report, in that cell size did not correlate with cilium length in wildtype P14 ($R^2 = 0.014$) or P31 ($R^2 = 0.28$) across regions (Fig. 5).

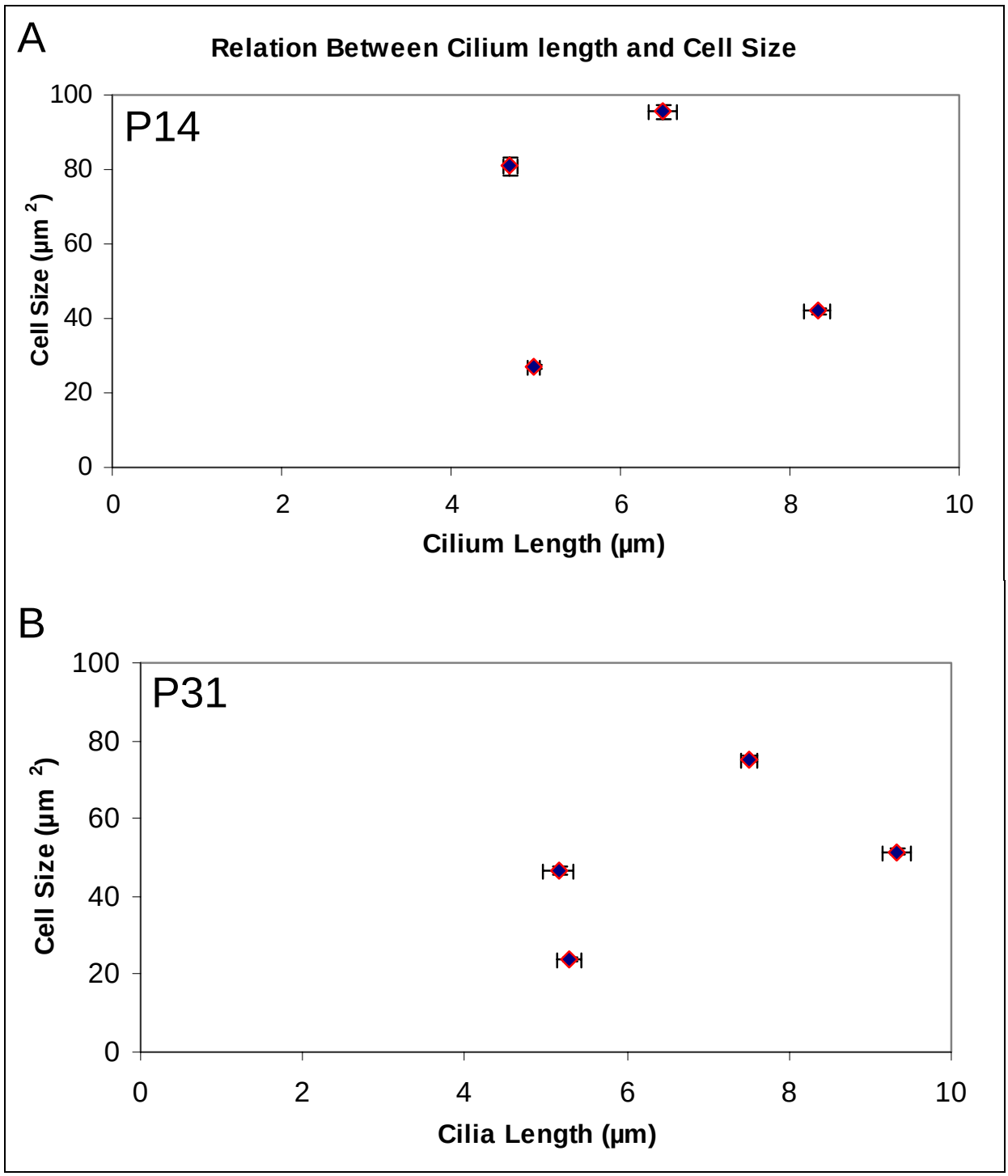

Figure 5. There was no apparent correlation between neuronal cell size and neuronal cilium length on P14 (R = 0.014) (A) or on P31(R = 0.281)(B).

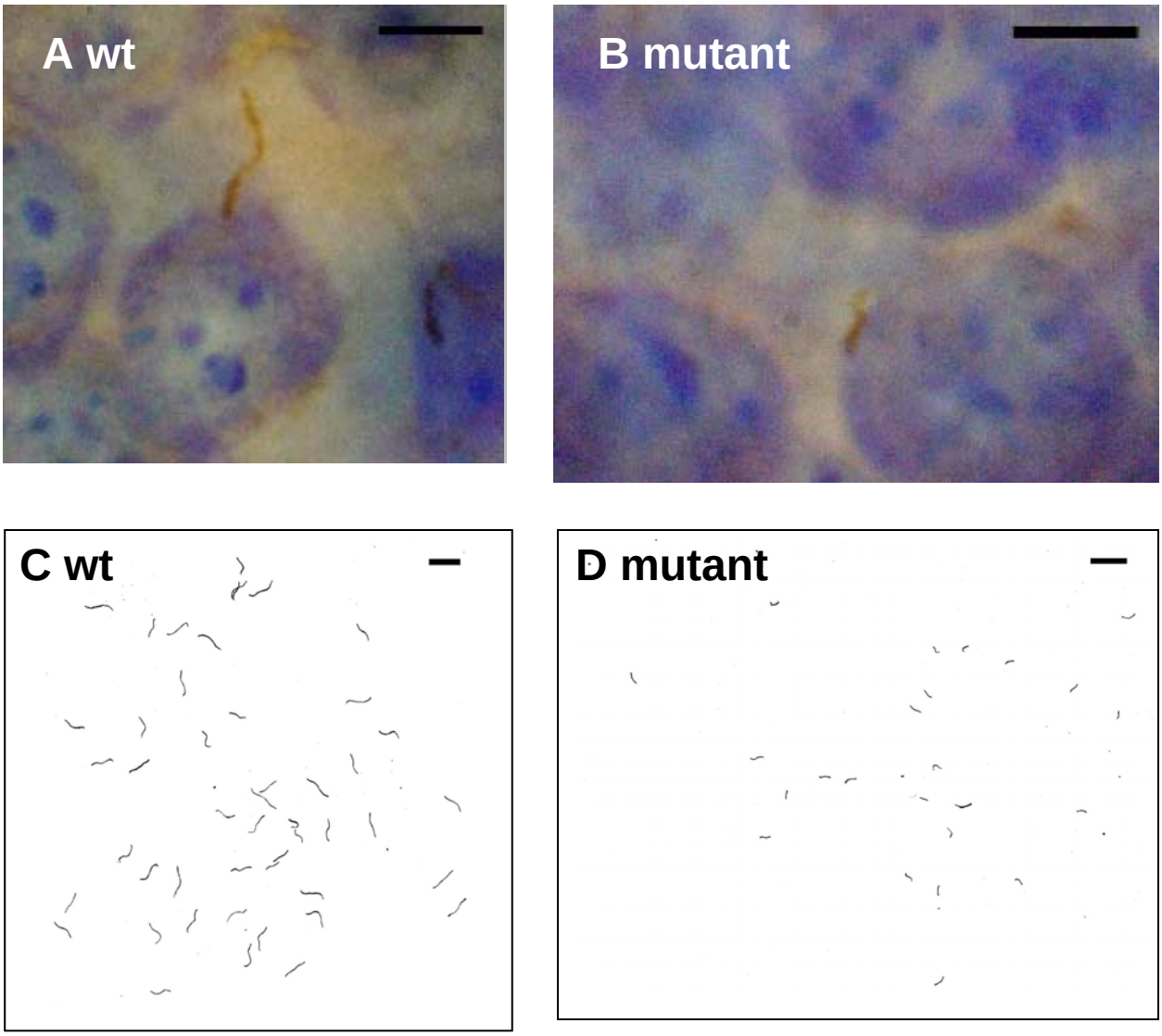

Figure 6. Neuronal cilia from layer 2 of piriform cortex, P31were immunostained for sst3 (brown), and the cells were counterstained with thionin (blue), which stains DNA and Nissl substance (A,B). Cilium length was significantly reduced from $Tg737^{orpk}$(wt) (A) to $Tg737^{orpk}$(-/-) (B). Cilia drawn with the aid of a cameral lucida. A marked numerical reduction was observed in ciliated neurons in from Wildtype (C) to Mutant (D). Scale bars, 5µm.

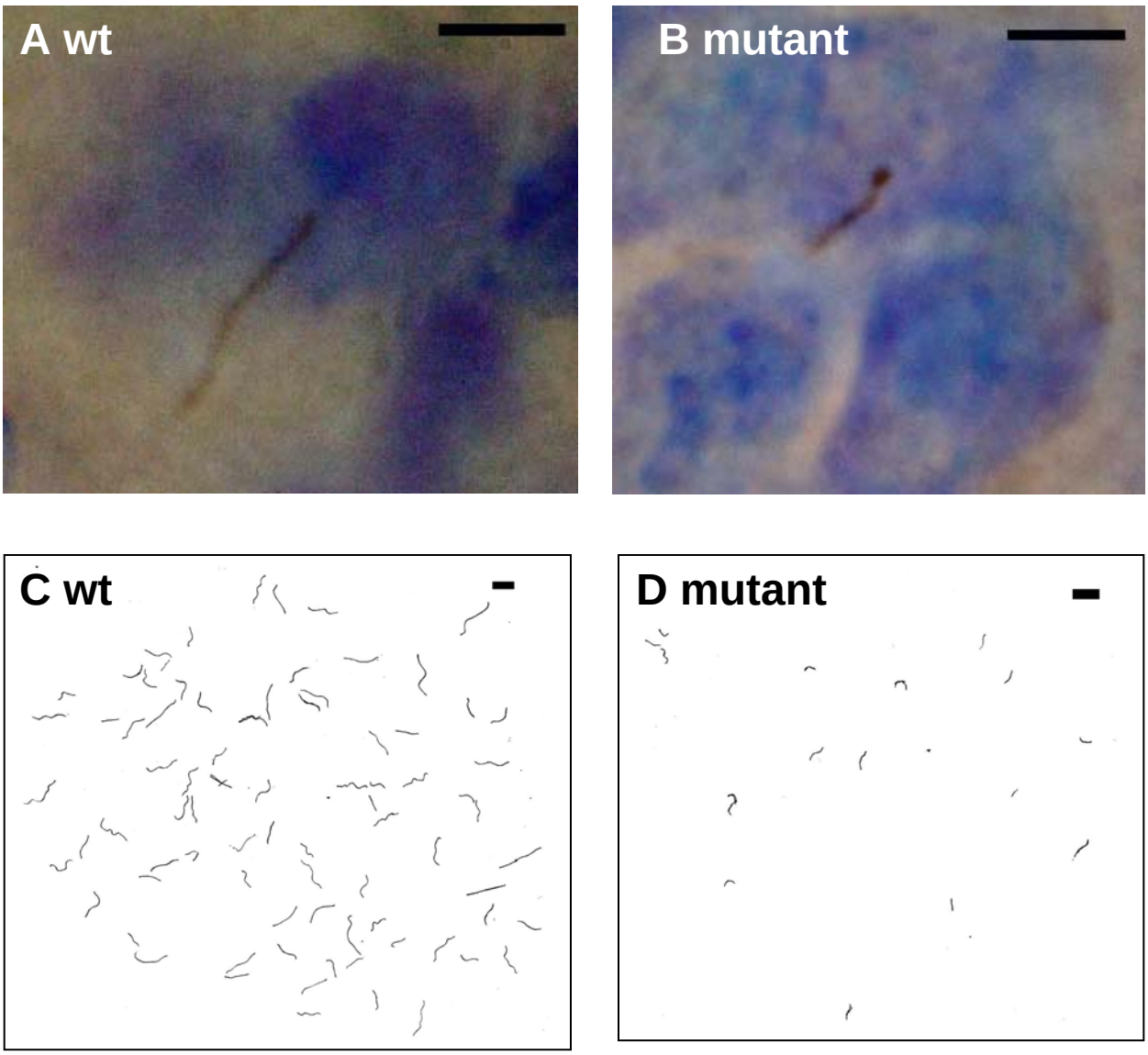

Figure 7. In the P31 VMH, cilium length was significantly reduced in the mutant. (A) Tg737^{orpk}(wt) (B) Tg737^{orpk}(-/-) (B). Numerical density was also greatly reduced as shown by comparing (C) Tg737^{orpk}(wt) to (D) Tg737^{orpk}(-/-). Scale bars, 5µm.

29

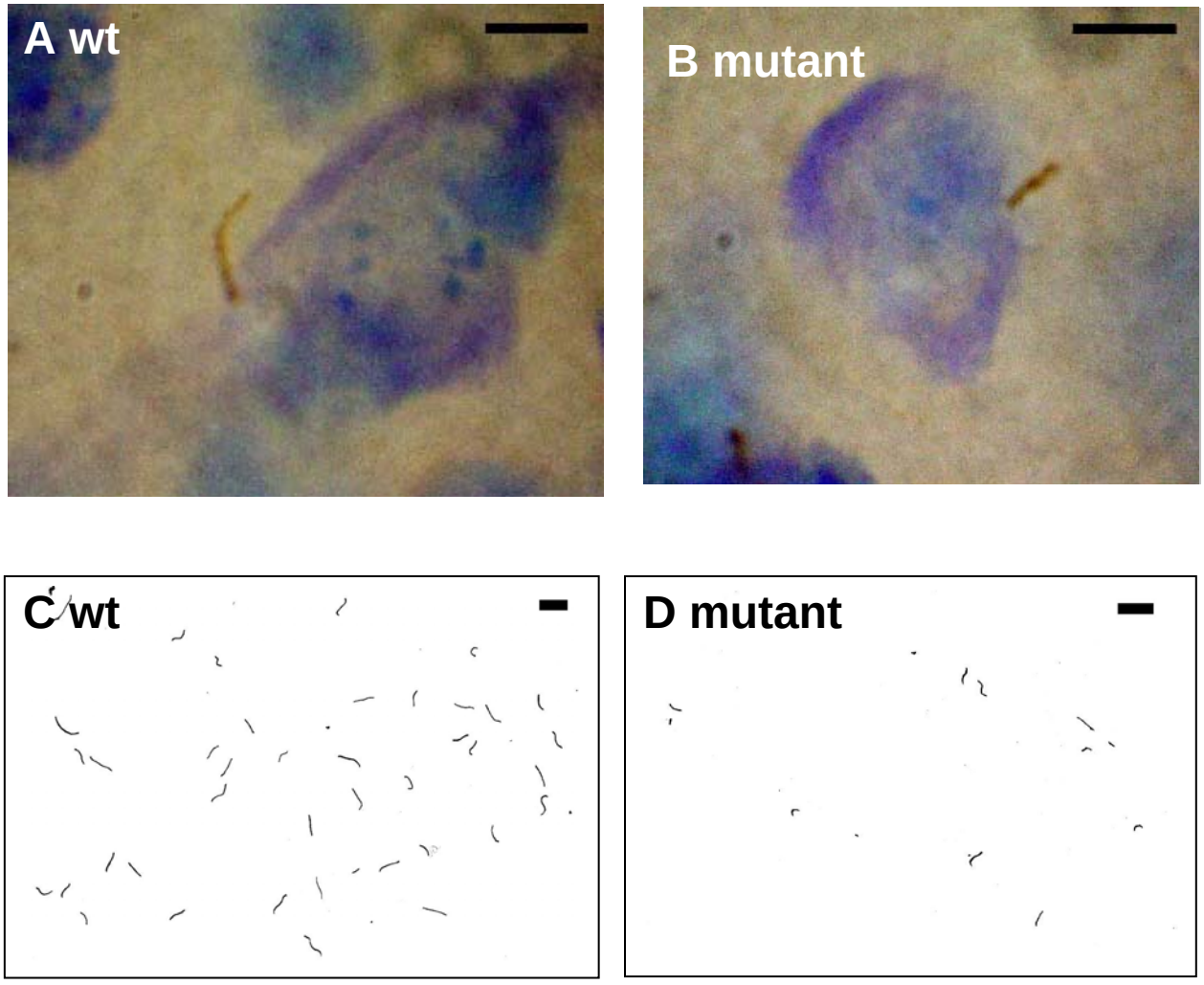

Figure 8. In the P31 hilus of the dentate gyrus, cilium length was significantly reduced. (A) Tg737^{orpk}(wt) (B) Tg737^{orpk}(-/-) (B).The numerical density of cilia was also greatly reduced as shown by comparing (C) and (D). Scale bars, 5µm.

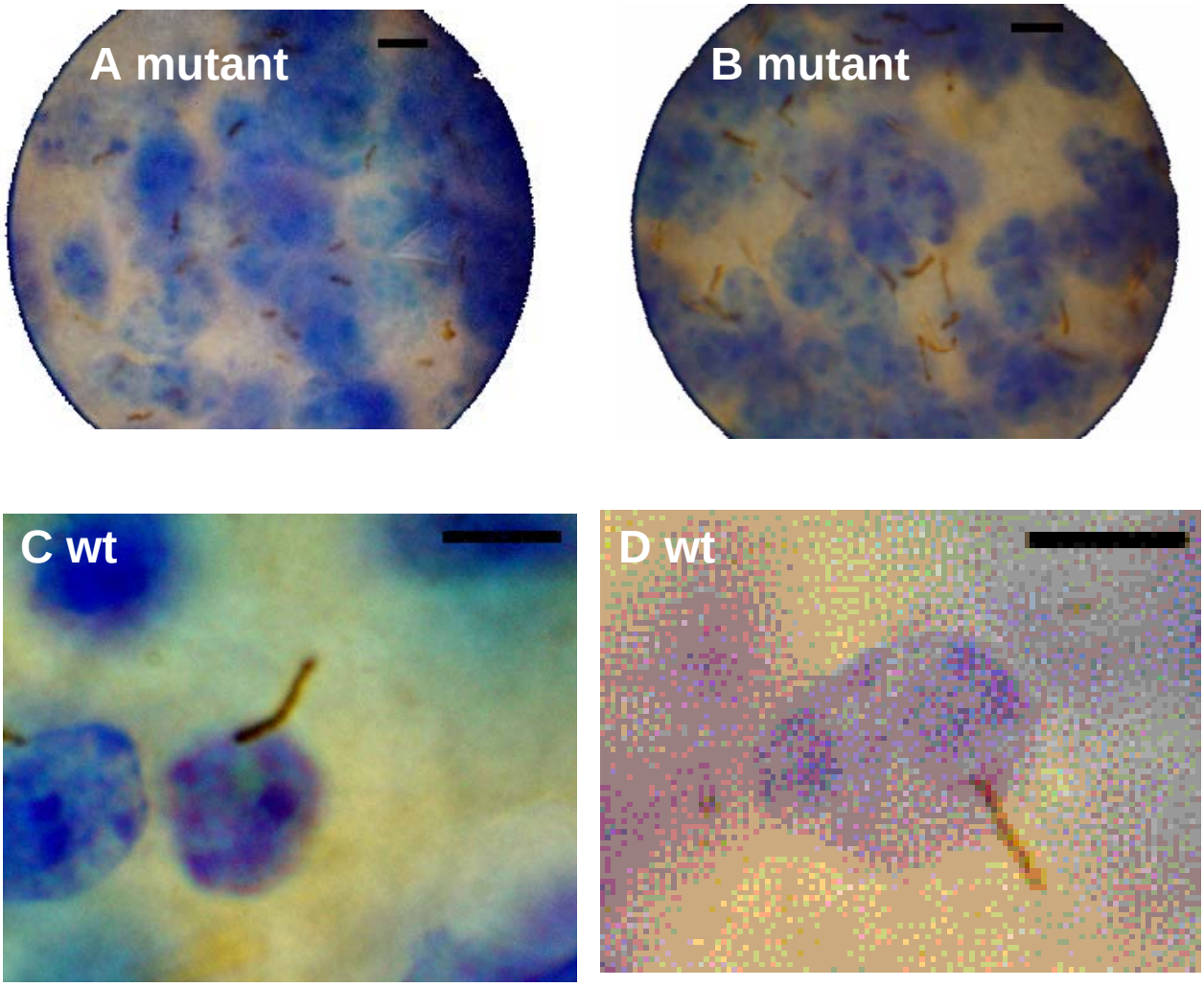

Figure 10. The Tg737^{orpk} mutation affected cilium length in IPL region (A) Tg737^{orpk}(-/-) (B) Tg737^{orpk}(wt) and in GrL (C) Tg737^{orpk}(-/-) (D) Tg737^{orpk}(wt). A, B scale bar 3 μm and C, D scale bars 5 μm.

DISCUSSION

The role of primary cilia has remained elusive. Primary cilia can only be localized with labor-intensive electron microscopy or with immunohistochemistry with a few known antibodies. A study of cilia in the epithelial lining of kidney tubules in Tg737^{orpk} mutant mice has revealed that they may sense the chemical milieu of tubular fluid (Nauli et al. 2003). Since the Tg737^{orpk} mutation causes stunting of cilia in kidney tubules, the mice develop polycystic kidney disease. These mice do not initially have polycystic kidney disease, but develop it after postnatal day 8 (Gresh et al. 2004). In this study, we have shown that the Tg737^{orpk} mutation also affected cilia morphology throughout the brain. In the fifty brain regions that were surveyed, it appears that the polaris mutation hinders cilia maintenance in almost all regions.

As is the case in renal cells (Pazour et al. 2000), the polaris mutation had a larger effect on neurons as the animals age. We have quantitatively demonstrated that in both age groups (P14 and P31), cilia were markedly shorter in Tg737^{orpk} mutant compared to wildtype in all of the six regions that were quantified. Numerical density of cilia also decreased significantly in those regions. Furthermore, the polaris mutation had considerably larger impact at P31 than P14, with the exception of IPL and GrL of the olfactory bulb. While the mutation decreased cilium length by an average of 39.2% in the six brain regions surveyed on P14, it decreased cilium length by an average of 49.2% in P31. Furthermore, the percentage of ciliated neurons was reduced by an average of 42.9% compared to the wildtype in P14, while it was reduced by an average of 71.9% when compared to the wildtype in P31. Since the polaris mutation appears to

affect P31 more severely than P14, the role of polaris may be to maintain cilia rather than ciliogenesis.

In addition, there was no correlation between mean cell size and cilia length on either P14 or P31 across regions. We did not assess cell size and cilia length within regions. Finally, we have found that the polaris mutation had a larger impact on cilium length in IPL of the olfactory bulb than in the GrL of olfactory bulb. While the cilia length was reduced by an average of 15.8% in the GrL, the cilia length in IPL was reduced by an average of 48.4% (Table 3).

The reason for the progressive shortening of cilia with age is unknown. One possibility is that since the polaris mutation causes a defect in IFT (Murcia et al. 2000), the defective IFT system leads to a decrease in monomer (alpha tubules and beta tubules) transport to the tip. Microtubules are in continuous dynamic equilibrium, with continuous polymerization and depolymerization of microtubules. Polymerization of microtubules is dependent on the concentration of free monomers available at its tip, but depolymerization is not dependent on concentration of free monomers (Desai and Mitchison 1997). When the concentration of free monomers is above critical concentration (C_c) there are more monomers added onto the polymer end than monomers leaving. Thus the cell thermodynamically favors polymerization. However, if the concentration of free monomers is below the critical concentration, then there are less monomer added than monomers leaving the polymer end and thus the cell thermodynamically favors depolymerization (Mitchison and Kirschner 1984). In *Chlamydomonas*, it was shown that flagella are dynamic structures by visualizing tubulin assembling and disassembling continuously at the distal end of the flagella (GFP

tagged β-tubulin, Marshall and Rosenbaum 2001). Most cilia are in a state where the concentrations of free monomers are at or above critical concentration; therefore, they are at equilibrium. Consequently, when the IFT is defective, the concentration of free monomers decreases at the apical tip, which favors the microtubules to depolymerize.

It has been shown that Tg737 gene can be expressed in different forms via alternative splicing (Taulman et al. 2001). Therefore it is possible that the cell produces two different types of polaris: one that functions completely and one that functions only partially. Early in the development the cell may splice the Tg737 gene to produce fully functioning polaris for ciliogenesis, since the concentration of monomers needs to be greater than critical concentration ($C > C_c$). Later in the development, it may produce partially functioning polaris for maintaince, since the concentration of monomers needs to be equal to the critical concentration ($C = C_c$). It is also conceivable that $Tg737^{orpk}$ mutation affects the partially functioning polaris splice variant while sparing fully functional polaris. Therefore, as the mice age, cells might produce more non-functioning polaris, causing concentration of monomers to decrease ($C < C_c$), which in turn leads to shorter microtubules and thus shorter cilia.

In addition to the decreases in length, there were dramatic reductions in the numerical density and percentage of ciliated neurons in $Tg737^{orpk}$(-/-). This might be due to a lack of centrosomal γ-tubulin (cultured neurons, Leask et al. 1997). As described above, the defect in IFT should result in depletion of free monomers, which thermodynamically favors microtubules to depolymerize. In order for cilia to grow back, the microtubules must polymerize once again. Although one α-tubulin and one β-tubulin can spontaneously assemble, γ-tubulin is necessary for the 13 monomers to assimilate

in order to form a nucleus (Evans et al. 1978) that serves as a foundation for microtubule assembly. Since centrosomes are deficient in γ-tubulin, this may halt microtubules from polymerizing in centrosomes (basal bodies) where cilia are born.

In addition, while we have determined the length of cilia in each region, it must be noted that there are several different types of neurons present in each region. Furthermore, as mentioned above, since polaris gene undergoes alternative splicing, the degree of functional polaris produced could be dependent on cell type. There may be particular cell types that produce a completely non-functional polaris and therefore are drastically affected in terms of the presence and cilia length, while there may be some type of cells that produce a completely functional polaris and therefore are unaffected by the polaris mutation. In addition, while the polaris mutation affects cilia length, reasons for regional differences in the extent of the defect remains to be determined.

Finally, it must be noted that cilia length in the IPL is affected more severely than the GrL of olfactory bulb. Although the explanation is unknown, my hypothesis is that the polaris mutation affects older cells more than younger, and perhaps less differentiated cells. The olfactory bulb continues to receive new neurons from subventricular layer via rostral migratory stream throughout adulthood (Luskin 1993). These stem cells enter the olfactory bulb through the GrL and migrate radially to differentiate into the IPL (Liu and Yi 2003). Since the GrL continues to receive new stem cells, this might be the reason why cilium length is not as affected by the polaris mutation as it is in other regions.

Although there were no significant differences in cell size between Tg737^{orpk}(wt) and Tg737^{orpk}(-/-), overall there were a dramatic changes in the morphology of the brain. A hallmark of Tg737^{orpk}(-/-) mice is that they have hydrocephalis (Taulman et al. 2001) and thus may have fewer neurons than wildtype. The exact explanation for hydrocephalis is still debatable; however, it has been noted that the polaris mutation does in fact cause the ventricles to enlarge, encroaching into neuron territory. Of the six regions that were extensively studied, the VMH was most affected by the polaris mutation. On P31 the cilium length decreased by 57.6% and by 80.4% in percentage of ciliated neurons. It is possible that it is related to hydrocephalus, as the ventromedial hypothalamus is in close proximity to the third ventricle.

The observation that the polaris mutation caused decreased cilia length and percentage of ciliated neurons suggests that intraflagellar transport involving polaris is necessary for maintaince of neuronal cilia, as is the case in kidney and other organs. Since cilia length and numerical cilia density showed greater reductions on P31 compared to P14, it is likely that polaris is involved in maintaince of the neuronal cilia more than in ciliogenesis. The observation that cilia length was less affected in GrL than in IPL of the olfactory bulb is compatible with the hypothesis that the progression of the defect depends at least partially on the age of the cell. Furthermore, the regional heterogeneity in the effect of polaris mutation on neuronal cilia suggests that the functions of some brain regions such as the VMH might be more compromised than others, such as the GrL.

REFERENCES

Allen, R.A. 1965. Isolated cilia in inner retinal neurons and in retinal pigment epithelium. *J. Ultrastruct Res.* 12:730–747.

Dahl, H.A. 1963. Fine structure of cilia in rat cerebral cortex. *Z. Zellforsch. Mikrosk. Anat*. 60:369–386.

Desai, A., Mitchison, T.J. 1997. Microtubule polymerization dynamics. *Annu. Rev. Cell Dev. Biol.* 13:83-117.

Dutcher, S.K. 1995. Flagellar assembly in two hundred easy-to-follow steps. *Trends. Genet.* 11:398-404.

Fuchs, JL., Schwark, H.D. 2004. Neuronal primary cilia: a review. *Cell Biol. Intl.* 28:111-1118.

Evans, L., Mitchison, T., Kirschner, M. 1985. Influence of the centrosome on the structure of nucleated microtubules. *J. Cell Biol.* 100:1185–91.

Gresh, L., Fischer, E., Reimann, A., Tanguy, M., Garbay, S., Shao, X., Hiesberger, T., Fiette, L., Igarashi, P., Yaniv, M., Pontoglio, M. 2004. A transcriptional network in polycystic kidney disease. *EMBO J*. 23:1657-1668.

Haycraft, C.J., Swoboda, P., Taulman, P.D., Thomas, J.H., Yoder, B.K. 2001. The C. elegans homolog of the murine cystic kidney disease gene Tg737 functions in a ciliogenic pathway and is disrupted in osm-5 mutant worms. *Development* 128:1493-1505.

Händel, M., Schulz, S., Stanarius, A., Schreff, M., Erdtmann-Vourliotis, M., Schmidt, H. 1999. Selective targeting of somatostatin receptor 3 to neuronal cilia. *Neuroscience* 89:909–926.

Hughes, R. Runyan, A.M, Fuchs, J.L, Schwark, H.D. 2002. Neuronal cilia: a morphometric study*. Soc Neurosci Abstr*. 28.

Leask, A., Obrietan, K., Stearns, T. 1997. Synaptically coupled central nervous system neurons lack centrosomal γ-tubulin. *Neurosci. Lett.* 229:17-20.

Liu, G., Yi, R. 2003. Neuronal Migration from the forebrain to the olfactory bulb requires a new attractant persistent in the olfactory bulb. *J. Neurosci*. 23(16):6651-6659

Luskin, M.B. 1993. Restricted proliferation and migration of postnatally generated neurons derived from the forebrain subventricular zone. *Neuroscience* 11:173–189.

Kozminski, K.G., Johnson, K.A., Forscher, P., Rosenbaum, J.L. 1993. A motility in the eukaryotic flagellum unrelated to flagellar beating. *Proc. Nat. Acad. Sci. USA* 90:5519-5523.

Karlsson, U. 1966. Three-dimensional studies of neurons in the lateral geniculate nucleus of the rat. I. Organelle organization in the perikaryon and its proximal branches. *J. Ultrastruct. Res.* 16:429–481.

Moyer, J.H., Lee-Tischler, M.J., Kwon., Schrick, J.J., Avner, E.D., Sweeney, W.E., Godfrey, V.L., Cacheiro, N.L.A., Wilkinson, J.E., Woychik, R.P. 1994. Candidate gene associated with a mutation causing recessive polycystic kidney disease in mice. *Scence* 264:1329-1333.

Marshall, W.F., Rosenbaum, J.L. 2001. Intraflagellar transport balances continuous turnover of outer doublet microtubules: implications for flagellar length control. *J. Cell Biol.* 155:405–414.

Marszalek, J.R., Ruiz-Lozano, P., Roberts, E., Chien, K.R., and Goldstein, L.S. 1999. Situs inversus and embryonic ciliary morphogenesis defects inmouse mutants lacking the KIF3A subunit of kinesin-II. *Proc. Natl. Acad. Sci. USA* 96:5043-5048.

Mitchison, T., Kirschner, M. 1984. Dynamic instability of microtuble growth. *Nature* 312:237-242.

Murcia, N.S., Richards, W.G., Yoder, B.K., Mucenski, M.L., Dunlap, J.R., Woychik, R.P. 2000. The Oak Ridge Polycystic Kidney (orpk) disease gene is required for left-right axis determination. *Developement* 127:2347–2355.

Nakanishi, K., Sweeney,W.E., Avner, A.D., Murcia, N.S. 2001. Expression of the orpk disease gene during kidney development and maturation. *Pediatr. Nephrol.* 16:219-226.

Nauli, S.M., Alenghat, F.J., Luo, Y., Williams, E., Vassilev, P., Li, X., Elia, A.E.H., Lu, W., Brown, E.M., Quinn, S.J., Ingber, D.E., Zhou, J. 2003. Polycystins 1 and 2 mediate mechanosensation in the primary cilium of kidney cells. *Nat. Genet.* 33:129–137.

Newby, L.J., Streets, A.J., Zhao, Y., Harris, P.C., Ward, C.J., Ong, A.C. 2002. Identification, characterization, and localization of a novel kidney polycystin-1-polycystin-2 complex. *J. Biol. Chem*. 277:20763-20773.

Nonaka, S., Tanaka, Y., Okada, Y., Takeda, S., Harada, A., Kanai, Y., Kido, M., Hirokawa, N. 1998. Randomization of left-right asymmetry due to loss of nodal cilia generating leftward flow of extraembryonic fluid in mice lacking KIF3B motor protein. *Cell* 95:829-37.

Pazour, G.J., Wilkerson, C.G., Witman, G.B. 1998. A dynein light chain is essential for the retrograde particle movement of intraflagellar transport (IFT). *J. Cell Biol.* 141:979-992.

Pazour, G.J., Dickert, B.L., Witman, G.B. 1999. The DHC1b (DHC2) isoform of cytoplasmic dynein is required for flagellar assembly. *J. Cell Biol.* 144:473–481.

Pazour, G.J., Dickert, B.L., Vucica, Y., Seeley, E.S., Rosenbaum, J.L., Witman, G.B., Cole, D.G. 2000. Chlamydomonas IFT88 and its mouse homologue, polycystic kidney disease gene *Tg737*, are required for assembly of cilia and flagella. *J. Cell Biol.* 151:709–718.

Pazour, G.J., Baker, S.A., Deane, J.A., Cole, D.G., Dickert, B.L., Rosenbaum, J.L., Witman, G.B., Besharse, J.C. 2002. The intraflagellar transport protein, IFT88, is essential for vertebrate photoreceptor assembly and maintenance. *J. Cell. Biol.* 157:103-113.

Pazour, G.J. 2004. Intraflagellar transport and cilia-dependent renal disease: the ciliary hypothesis of polycystic kidney disease. *J. Am. Soc. Nephrol.* 15:2528-2536.

Peters, A., Palay, S.L., Webster, H.D. 1976. *The fine structure of the nervous system: neurons and their supporting cells,* W.B. Saunders Co, Philadelphia.

Praetorius, H.A., Spring, K.R. 2001. Bending the MDCK cell primary cilium increases intracellular calcium. *J. Mem. Biol*. 184:71-79.

Rosenbaum, J.L., Cole, D.G., Diener, D.R. 1999. Intraflagellar transport: the eyes have it. *J. Cell Biol.* 144:385-388.

Schweitzer, P., Madamba, S., Champagnat, J., Siggins, G.R. 1993. Somatostatin inhibition of hippocampal CA1 pyramidal neurons: mediation by arachidonic acid and its metabolites. *J. Neurosci.* 13:2033-2049.

SAS Institute Inc. 1996. SAS System for Windows. Release 9.1. SAS, Cary, NC.

Taulman, P.D., Haycraft, C.J., Balkovetz, D.F., Yoder, B.K. 2001. Polaris, a protein involved in left-right axis patterning, localizes to basal bodies and cilia. *Mol. Biol. Cell* 12:589–599.

Whitfield, J.F. 2004. The neuronal primary cilium-an extrasynaptic signaling device. *Cell Signal.* 16:763-767.

Yoder, B.K., Richards, W.G., Sweeney, W.E., Wilkinson, J.E., Avener, E.D., Woychik, R.P. 1995. Insertional mutagenesis and molecular analysis of a new gene associated with polycystic kidney disease. *Proc. Assoc. Am. Phys*. 107:314-323.

Yoder, B.K., Tousson, A., Millican, L., Wu, J.H., Bugg Jr, C.E., Schafer, J.A. et al. 2002. Polaris, a protein disrupted in orpk mutant mice, is required for assembly of renal cilium. *Am. J. Physiol. Renal Physiol.* 282:F541–F552.